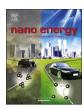
FISEVIER

### Contents lists available at ScienceDirect

# Nano Energy

journal homepage: www.elsevier.com/locate/nanoen



# Full paper

# Encapsulating MnO nanoparticles within foam-like carbon nanosheet matrix for fast and durable lithium storage



Yu-Chen Xiao<sup>a,b</sup>, Cheng-Yan Xu<sup>a,b,\*</sup>, Pan-Pan Wang<sup>a,b</sup>, Hai-Tao Fang<sup>a</sup>, Xue-Yin Sun<sup>a</sup>, Fei-Xiang Ma<sup>a,b</sup>, Yi Pei<sup>a,b</sup>, Liang Zhen<sup>a,b,\*</sup>

- <sup>a</sup> School of Materials Science and Engineering, Harbin Institute of Technology, Harbin 150001, China
- b MOE Key Laboratory of Micro-System and Micro-Structures Manufacturing, Harbin Institute of Technology, Harbin 150080, China

#### ARTICLE INFO

#### Keywords: Lithium ion batteries Anode materials MnO Carbon framework Internal voids

#### ABSTRACT

Long-life MnO-based anodes with high power density for lithium ion batteries (LIBs) is still a great challenge due to the inferior electrical conductivity and drastic volume change of MnO during the lithiation/delithiation process. Herein, to achieve high rate capacity and long cycle life simultaneously, MnO nanoparticles were encapsulated within a foam-like carbon nanosheet matrix through a confined phase transition process. By annealing polydopamine (PDA) coated porous ZnMnO $_3$  nanosheets in a reducing atmosphere, MnO nanoparticles and surrounding *in-situ* formed pores could be encapsulated in the PDA-derived carbon nanosheets synchronously, forming MnO@C nanosheets with ball-in-pore structure (MnO@C-BP). The internal voids originating from Zn evaporation can not only accommodate the huge volume expansion of MnO nanoparticles, but also significantly enlarge the specific surface area, leading to an enhanced pseudocapacitive Li-storage behavior. Moreover, the as-prepared sheet-shaped MnO@C-BP with thickness of about 30 nm can provide a short path for fast Li-ion diffusion, while the continuous carbon framework promotes the charge transfer between the encapsulated MnO nanoparticles. Because of these merits, MnO@C-BP electrode exhibits superior rate performance (514 mAh g $^{-1}$  at  $10 \text{ Ag}^{-1}$ , 383 mAh g $^{-1}$  at  $15 \text{ Ag}^{-1}$ ), outstanding cycling performance (1212 mAh g $^{-1}$  after 1000 cycles at  $2 \text{ Ag}^{-1}$ , capacity retention of 127%), as well as a high reversible capacity of 1178 mAh g $^{-1}$  at  $0.1 \text{ Ag}^{-1}$ .

# 1. Introduction

The ever-increasing performance demands for portable electronic devices and electric vehicles have stimulated significant interests in seeking advanced anode materials for next-generation lithium-ion batteries [1–3]. Transition-metal oxides (TMOs) stand out from various potential anode materials because of their high theoretical specific capacity, low cost and easy availability [4,5]. Among the intensively studied TMOs anodes such as Fe<sub>3</sub>O<sub>4</sub> [6], Co<sub>3</sub>O<sub>4</sub> [7], NiO [8], and MnO<sub>x</sub> [9,10], MnO has the lowest voltage hysteresis and discharge-charge potential (around 0.5-1.2 V vs Li/Li<sup>+</sup>) [4,11], as well as high density, and the advantage of nature abundance, which make it one of the most promising anode materials [12,13]. Nevertheless, like other TMOs, the main challenges associated with MnO are the inferior electrical conductivity and the drastic volume change (~171%) during the lithiation/delithiation process [14], leading to poor rate capability and short cycle life, impeding the successful implementation of MnO in commercial applications [15,16].

So far, to address the above drawbacks of MnO anodes, besides binding MnO with conductive carbon host (such as rGO [17,18], CNTs [19,20], etc), the most effective and low-cost approach is coating MnO with amorphous carbon [21–24]. It has been demonstrated that carbon coating can boost the electrical conductivity and prevent the MnO particles from agglomeration, however, the elastic feature of carbon layers could only partly relieve the strain caused by the huge volume change during lithiation/delithiation process, leading to unsatisfactory cycling performance [25,26]. Particularly, the specific capacity of MnO@C core-shell nanoplates [27] (prepared via deposition of acetylene with Mn(OH)<sub>2</sub> nanoplates) dropped from  $\sim 800 \, \text{mAh g}^{-1}$  to less than  $600 \, \text{mAh g}^{-1}$  after 30 cycles at  $0.1 \, \text{A g}^{-1}$ . Coaxial MnO/C nanorods [28] obtained using polypyrrole-coated MnOOH precursors were reported to be able to discharge/charge at 500 mAh g<sup>-1</sup> for 100 cycles. Actually, a serious structural failure of carbon shells (due to the repeating volume change of MnO cores) in MnO@C nanowires has been clearly observed by ex-situ transmission electron microscope (TEM) only after 100 discharge/charge cycles [26]. Therefore, it is a great

<sup>\*</sup> Corresponding authors at: School of Materials Science and Engineering, Harbin Institute of Technology, Harbin 150001, China. E-mail addresses: cy\_xu@hit.edu.cn (C.-Y. Xu), lzhen@hit.edu.cn (L. Zhen).

Y.-C. Xiao et al. Nano Energy 50 (2018) 675–684

challenge to fabricate MnO/C composite to achieve both high rate capacity and excellent long-term cycling performance.

In terms of preserving the structural integrity of MnO/C composites during long-term cycling, considerable efforts have been made on introducing void space inside the carbon shell to provide additional space for the volumetric expansion of MnO. Yolk-shell MnO<sub>x</sub>/C nanorods [29] were synthesized using SiO<sub>2</sub> as template for the void space, which exhibited a capacity of 634 mAh g<sup>-1</sup> after 900 cycles at a current density of 0.5 A g<sup>-1</sup>. Peapod-like MnO@C nanowires with internal void space were prepared through the deep reduction process of MnO2 cores [15,26]. The peapod-like MnO@C nanowires possess much improved cycling performance than core-shell MnO/C nanowires. Our group also reported the construction of volk-shell MnO/C nanodiscs through carbothermal reduction process [30]. The MnO/C nanodiscs delivered a specific capacity of 605 mAh g<sup>-1</sup> after 600 cycles at 1 A g<sup>-1</sup>. These above reports have demonstrated the key role of void space on avoiding the fractures of carbon layers and stabilizing the solid electrolyte interphase (SEI) to improve the structural stability of the electrode. However, as shown in Fig. S1a, due to the large void space in the yolkshell structure, the point to point contact between MnO core and carbon shell may retard the fast transport of electrons from carbon to the active materials, leading to unsatisfactory rate performance [31,32]. In contrast, multicore-shell MnO@C structure [24,33] (MnO@C-MCS) could provide a large core-shell contact area, and the carbon framework could act as 3D conductive network for electrons (Fig. S1b), which contributed to enhanced rate performance. However, there is no additional void space for the volume expansion of MnO in such structure, the repeating volume variation may lead to less competitive cycling performance [34,35]. Therefore, novel MnO@C composite with suitable internal voids and better core-shell contact is much needed for achieving both high rate capacity and long life span.

In this work, we design a unique ball-in-pore (BP) structure for MnO/C anode, and demonstrate the stepwise fabrication of MnO@C nanosheets with ball-in-pore structure (MnO@C-BP) by encapsulating MnO nanoparticles within foam-like carbon nanosheets. As shown in Fig. S1c, the BP structure combines the structural advantages of yolk-shell structure (Fig. S1a) and multicore-shell structure (Fig. S1b). On the one hand, comparing with yolk-shell structure, BP structure also has suitable internal voids to accommodate the volume expansion, while the core-shell contact area of BP structure is higher due to its multipoint contacts. On the other hand, BP structure still possesses 3D conductive network as multicore-shell structure. Moreover, the significantly enlarged specific surface area due to the abundant internal voids could contribute to enhanced pseudocapacitive Li-storage behavior. As expected, this unique BP structure endows MnO@C-BP with remarkable electrochemical performance as an anode material for LIBs.

## 2. Experimental section

# 2.1. Materials synthesis

# 2.1.1. $Zn_{0.5}Mn_{0.5}C_2O_4$ ·EG nanosheets

In a typical procedure,  $3\,\text{mmol}$  MnAc<sub>2</sub>·4H<sub>2</sub>O and  $3\,\text{mmol}$  ZnAc<sub>2</sub>·2H<sub>2</sub>O were dissolved in 10 mL ethylene glycol (EG) to make solution A. 6 mmol oxalic acid and 1 g PVP were dissolved in 90 mL water/EG (1:8) mixed solvent to make solution B. Then, solution A was quickly added into solution B under stirring. The obtained mixture was kept under stirring at ambient temperature for 1 h. The white precipitates (Zn<sub>0.5</sub>Mn<sub>0.5</sub>C<sub>2</sub>O<sub>4</sub>·EG) were collected by centrifugation, washed three times with absolute alcohol and dried in an oven.

# 2.1.2. Porous ZnMnO3 nanosheets

Porous ZnMnO $_3$  nanosheets were prepared by annealing Zn $_{0.5}$ Mn $_{0.5}$ C2O $_4$ :EG at 400  $^{\circ}$ C for 2 h in air.

#### 2.1.3. MnO@C-BP

The as-prepared ZnMnO<sub>3</sub> nanosheets (0.4 g) were first dispersed in 200 mL de-ionized water, followed by adding 200 mg dopamine (DA), and stirring for 60 min for the diffusion of DA molecules into the pores of the as-prepared porous ZnMnO<sub>3</sub>. Then, 0.242 g 2-amino-2-hydroxymethyl-1,3-propanediol (Tris) was added into the mixture to start the polymerization (pH value increased to about 8.5). The polymerization was allowed to proceed for 12 h. Then polydopamine coated ZnMnO<sub>3</sub> (ZnMnO<sub>3</sub>@PDA) was collected by centrifugation, washed several times with de-ionized water and ethanol, then dried in air. Finally, MnO@C-BP was obtained by heating ZnMnO<sub>3</sub>@PDA at 700 °C for 3 h under flowing H<sub>2</sub>/Ar gas (5% H<sub>2</sub>). For comparison, multicore-shell MnO@C composite (MnO@C-MCS) without large internal voids were also synthesized by replacing 3 mmol MnAc<sub>2</sub>·4H<sub>2</sub>O and 3 mmol ZnAc<sub>2</sub>·2H<sub>2</sub>O with 6 mmol MnAc<sub>2</sub>·4H<sub>2</sub>O at the first step, and the parameters of following procedures were identical to those of MnO@C-BP.

# 2.2. Materials characterization

The crystal structures were identified by means of X-ray diffraction (XRD) with Rigaku D/max 2500 diffractometer with Cu  $K_{\alpha}$  radiation ( $\lambda=0.15418$  nm). The morphologies and microstructures of the products were characterized by a field-emission scanning electron microscope (FE-SEM, FEI Quanta 200 F) and a transmission electron microscope (TEM, FEI Tecnai  $G^2$  F30). The MnO contents in the composites were measured by thermo-gravimetric analysis (TGA, NETzsch TG 209F3) at a ramping rate of  $10\,^{\circ}\text{C/min}$  in air. Nitrogen adsorption-desorption isotherms were performed on a Micrometrics ASAP 2020. X-ray photoelectron spectroscopy (XPS) spectra were performed on ESCALAB MK II X-ray photoelectron spectrometer. Raman spectra were recorded by Renishaw invia Raman microscope (532 nm laser for excitation).

# 2.3. Electrochemical measurements

Electrochemical test was performed using CR-2025 coin cells assembled in argon-filled glovebox. Li foil was used as reference electrode and the electrolyte was LiPF<sub>6</sub> in ethylene carbonate (EC)/dimethyl carbonate (DMC) (1: 1, w/w). The working electrode was prepared by mixing active materials, acetylene black and polyvinylidene fuoride (PVDF) binder (in the weight ratio of 7: 2: 1) in N-methyl pyrrolidinone (NMP) to form a homogenous slurry, then the slurry was pasted onto Cu foil and placed in vacuum at 120 °C for 10 h before the coin-cell assembly. The loading mass of the active materials was about 0.5 mg/ cm<sup>2</sup>. The galvanostatic charge/discharge tests were conducted on a battery program-control test system (Land CT2001A) in the voltage range of 0.01-3 V. The specific capacities of the electrodes were calculated based on the total mass of active materials including MnO and carbon. Cyclic voltammetry (CV) and electro-chemical impedance spectroscopy (EIS) were performed on a Chi 660E electrochemical workstation. CV measurements were recorded between 3 V and 0.01 V at a scan rate of 0.02 mV s<sup>-1</sup>. EIS were collected at frequencies ranging from 100 kHz to 0.01 Hz. All tests were performed at room temperature.

### 3. Results and discussion

Fig. 1a illustrates the synthetic procedure of MnO@C-BP. Briefly, MnO@C-BP could be obtained by annealing polydopamine (PDA) coated porous ZnMnO<sub>3</sub> nanosheets in a reducing atmosphere. In the synthesis, the PDA coating layers transform into porous carbon framework, and ZnMnO<sub>3</sub> converts into MnO nanoparticles encapsulated in the internal pores of carbon sheet. In detail, Zn<sub>0.5</sub>Mn<sub>0.5</sub>C<sub>2</sub>O<sub>4</sub>·(HOCH<sub>2</sub>CH<sub>2</sub>OH) (formulated as Zn<sub>0.5</sub>Mn<sub>0.5</sub>C<sub>2</sub>O<sub>4</sub>·EG) nanosheets (SEM image shown in Fig. 1b) were firstly prepared through a one-step co-precipitation process between zinc acetate, manganese acetate, and oxalic acid in ethylene glycol (EG) solution. XRD pattern of

# Download English Version:

# https://daneshyari.com/en/article/7952507

Download Persian Version:

https://daneshyari.com/article/7952507

<u>Daneshyari.com</u>